

RoboTSP – A Fast Solution to the Robotic Task Sequencing Problem

Francisco Suárez-Ruiz, Teguh Santoso Lembono and Quang-Cuong Pham

Abstract—In many industrial robotics applications, such as spot-welding, spray-painting or drilling, the robot is required to visit successively multiple targets. The robot travel time among the targets is a significant component of the overall execution time. This travel time is in turn greatly affected by the order of visit of the targets, and by the robot configurations used to reach each target. Therefore, it is crucial to optimize these two elements, a problem known in the literature as the Robotic Task Sequencing Problem (RTSP). Our contribution in this paper is two-fold. First, we propose a fast, near-optimal, algorithm to solve RTSP. The key to our approach is to exploit the classical distinction between task space and configuration space, which, surprisingly, has been so far overlooked in the RTSP literature. Second, we provide an open-source implementation of the above algorithm, which has been carefully benchmarked to yield an efficient, ready-to-use, software solution. We discuss the relationship between RTSP and other Traveling Salesman Problem (TSP) variants, such as the Generalized Traveling Salesman Problem (GTSP), and show experimentally that our method finds motion sequences of the same quality but using several orders of magnitude less computation time than existing approaches.

I. INTRODUCTION

In many industrial robotics applications, such as spot-welding, spray-painting or drilling, the robot is required to visit successively multiple targets. Consider for instance the drilling task depicted in Fig. 1, which was proposed at the Airbus Shopfloor Challenge held during ICRA 2016 in Stockholm, Sweden. The task, mimicking the actual drilling process in aircraft manufacturing, consisted in drilling as many holes as possible in one hour, from a given pattern of 245 hole positions. The robot travel time between the holes is a significant component of the overall execution time. This travel time is in turn greatly affected by the order of visit of the holes, and by the robot configurations used to reach each hole. Therefore, it is crucial to optimize these two elements, a problem known in the literature as the RTSP, see [1] for a recent review. Finally, note that, since the position of the panel is unknown at the beginning of the round, the planning time is included within the one hour limit. Thus, in this Challenge as in many practical applications, there is a need for an algorithm that can find near-optimal plans within minutes, not hours.

RTSP is closely related to TSP, a classical problem in Computer Science. In TSP, a set of locations is given on a map, and one is interested in finding the order to visit all the locations while minimizing the total travel distance, see Fig. 2 (a). The key difference between RTSP and TSP is that, in RTSP, each of the targets (e.g. a hole position) may

The authors are with the School of Mechanical and Aerospace Engineering, Nanyang Technological University, Singapore.

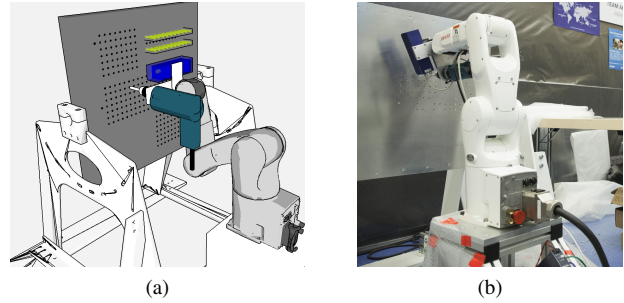


Fig. 1. The Airbus Shopfloor Challenge held during ICRA 2016. The task, mimicking the actual drilling process in aircraft manufacturing, consisted in drilling as many holes as possible, in one hour, from a given pattern of 245 hole positions. Since the position of the panel is unknown at the beginning of the round, the planning time is included within the one hour limit. a) The simulation environment. b) Our setup using a DENSO robot at the live Challenge, where our team won the second prize.

be reached by *multiple robot configurations*, also known as *Inverse Kinematics (IK) solutions*.

One simple work-around may consist in assigning a fixed robot configuration for each target: RTSP then becomes a classical TSP among the assigned robot configurations. Such a work-around is however sub-optimal. Another approach consists in formulating RTSP as an instantiation of GTSP: in GTSP, the locations are split into bins, and one is required to visit exactly one location per bin, see Fig. 2 (b). Here, each bin will contain the different robot configurations corresponding to the same target. While there have been many works devoted to GTSP and some efficient solutions exist, the sheer size of real-world RTSP instances¹ make this approach inapplicable in practice. Section II provides a more detailed discussion on existing approaches to solve RTSP.

Our contribution in this paper is two-fold. First, we propose a fast, near-optimal, algorithm to solve RTSP. The key to our approach is to exploit the classical *distinction between task space and configuration space*, which, surprisingly, has been so far overlooked in the RTSP literature. Specifically, we propose a three-step algorithm [see Fig. 2 (c) for illustration]:

- 1) Find a (near-)optimal visit order of the targets in a *task-space metric* (e.g. Euclidean distance between the hole positions), using classical TSP algorithms;
- 2) Given the order found in Step 1, find for each target

¹For instance, in the set-up of the Airbus Shopfloor Challenge, using a discretization of $\frac{\pi}{2}$ radians for the free-DoF, one obtains 3,779 different configurations, grouped into 245 bins, which cannot be solved in practical times by any existing GTSP solver. See also Section IV-D for a detailed comparison.

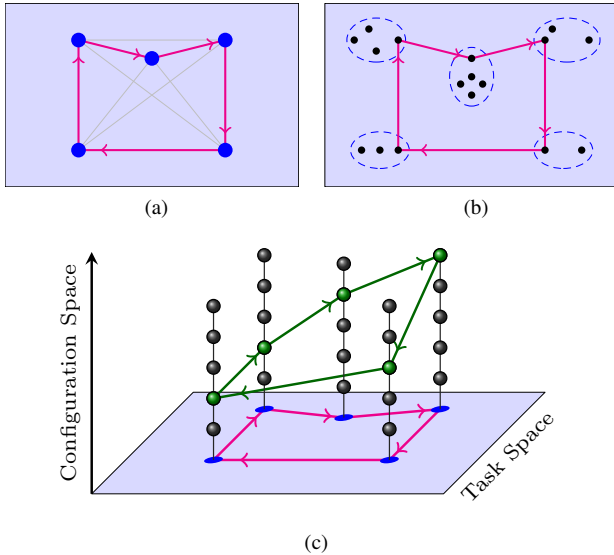


Fig. 2. (a) The Traveling Salesman Problem. (b) The Generalized Traveling Salesman Problem. (c) Decomposition of the Robotic Task Sequencing Problem into task-space and configuration-space.

the optimal robot configuration, so that the total path length through the configurations is minimized in a *configuration-space metric* (e.g. Euclidean distance between the robot configurations – collisions are ignored at this stage), using a graph shortest path search algorithm;

- 3) Compute the final collision-free configuration-space trajectories by running classical motion planning algorithms (e.g. Rapidly-Exploring Random Tree (RRT)) through the robot configurations found in Step 2 and in the order given by Step 1.

Our second contribution is to provide an open-source implementation² of the above algorithm. In particular, we carefully benchmark different key components of the algorithm (underlying task-space TSP solver, configuration-space metric, discretization step-size for the free-DoF), so as to come up with an efficient, ready-to-use, software solution.

The remainder of the paper is organized as follows. In Section II, we discuss existing approaches to RTSP. In Section III, we introduce and describe in detail the proposed method. In Section IV, we present the experimental results, showing in particular that our method finds motion sequences of the same quality but using several orders of magnitude less computation time than existing approaches. Finally, in Section V, we conclude with a few remarks.

II. RELATED WORKS

A recent survey on strategies to solve RTSP can be found in [1]. We recall some of the main results below.

In [2], the authors plan the motions for a 3-DoF robot to visit 6 targets, each of which can be reached with two

different robot configurations. For this, they formulate a GTSP with 6 bins and 2 configurations per bin. They then convert the GTSP into a TSP, which can be solved efficiently.

In [3], the authors consider a fruit picking task, which has up to 250 targets, but with only one robot configuration per target. The problem can then be directly formulated as a TSP, which the authors solved using the Nearest-Neighbor heuristic.

In [4], the authors consider a RTSP with one configuration per target, which can then be formulated as a regular TSP. The emphasis here is on collision-free trajectories, which are difficult to find when the environment includes obstacles. First, the authors approximate the travel cost between configurations as the Euclidean distance in the configuration space. Then, a minimum spanning tree is computed using Prim’s algorithm to find a near-optimal tour under the approximated cost. Next, collision-free paths are calculated given this near-optimal tour. The collision-free paths yield an updated travel cost, which is then used to iteratively refine the tour. This idea of computing first a good tour with a simple metric (without considering collisions) before computing collision-free trajectories is reused in our present work (but without the iterative refinement step).

An extension of this work is proposed in [5]. Here the authors consider multiple robot configurations per target. Instead of a spanning tree, they compute a near-optimal *group spanning tree* [6]. On a task involving 50 targets with 5 configurations per target, a near-optimal solution could be found in 9,600 s.

Following a different approach, the authors of [7] propose to use Genetic Algorithms (GAs) to solve GTSP. The optimization criteria is the task cycle time. On a task with 3-DoF and 6-DoF robots involving 50 targets, a near-optimal solution is found in 1,800 s. The quality of the solution depends on several control parameters (related to the GA) and the number of iterations. This approach has been further extended to include collision-free path planning for 2D and 3D environments [8], [9].

Yet another approach consists in formulating RTSP as a multi-objective constraint optimization problem. In [10], a robotic spray painting task is considered. The optimization criteria is set to minimize the task planning and execution time while maximizing the painting quality. Three constraints were defined: process, resources and quality constraints. The multi-objective problem then is solved using the Depth-First Search (DFS) algorithm. On a task involving 8 targets, with 4 configurations per target, an optimal solution is found in 10,000 s.

The main limitation of all the works discussed above is the large computation time they require. In particular, none of these works could have been applied to the setting of the Airbus Shopfloor Challenge presented in Section I, which involves 245 targets, with tens of configurations per target, and which has to be solved within a few minutes – since the planning time is counted in the one hour limit of the challenge.

²The open-source implementation of the proposed method is accessible at www.github.com/crigroup/robotssp

III. ROBOTSP ALGORITHM

A. Setting

Consider n targets in the task-space. A tour in the task-space that visits each target exactly once is called a *task-space tour*³. We first compute IK solutions for each target – using a suitable discretization for the free-DoFs if necessary. A tour in the configuration-space that starts from the robot “home” configuration, visits, for each target, exactly one IK solution associated with that target, and returns to the “home” configuration is called a *configuration-space tour*. Our objective is to find the fastest *collision-free* configuration-space tour subject to the robot constraints (e.g. velocity and acceleration bounds).

Let m_i be the number of IK solutions found for target i . If we do not take into account obstacles, there are $(n-1)! \left(\prod_{i=1}^n m_i \right)$ possible configuration-space tours (with straight paths) for this task. One cannot therefore expect to find the optimal sequence by brute force in practical times.

B. Proposed algorithm

As presented in Section I, our method consists in:

- 1) Finding a (near-)optimal task-space tour in a *task-space metric*;
- 2) Given the order found in Step 1, finding, for each target, the optimal robot configuration, so that the corresponding configuration-space tour has minimal length in a *configuration-space metric* – collisions are ignored at this stage;
- 3) Computing fast collision-free *configuration-space* trajectories by running classical motion planning algorithms (e.g. RRT-Connect with post-processing [11], [12]) through the configurations found in Step 2 and in the order given by Step 1.

Implementation details and benchmarking results for Steps 1 and 3 are given in Section IV.

Regarding Step 2, we first construct an undirected graph as depicted in Fig. 3. Specifically, the graph has n layers, each layer i contains m_i vertices representing the m_i IK solutions of target i (the targets are ordered according to Step 1), resulting in a total of $\sum_{i=1}^n m_i$ vertices. Next, for $i \in [1, \dots, n-1]$, we add an edge between each vertex of layer i and each vertex of layer $i+1$, resulting in a total of $\sum_{i=1}^{n-1} m_i m_{i+1}$ edges. Finally, we add two special vertices: “Start” and “Goal”, which are associated with the robot “home” configuration, and connected respectively to the m_1 vertices of the first layer and the m_n vertices of the last layer.

The edge costs are computed according to a configuration-space metric: for instance, the cost for the edge joining vertices q and q' can be given by the Euclidean distance in the configuration space $\sqrt{\sum_{k=1}^{\text{DoF}} (q_k - q'_k)^2}$. Section IV-B examines in detail how the choice of such metrics influences the quality of the final path. One can note here that the

³Strictly speaking, a tour requires to return to the first target, so we are making a slight abuse of vocabulary here.

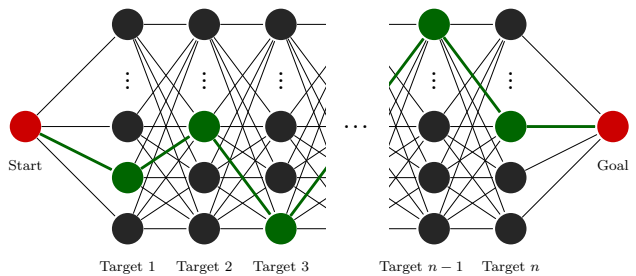


Fig. 3. Graph constructed for Step 2 of the algorithm. The targets are ordered according to Step 1. The shortest path (green lines) connecting the “Start” and “Goal” vertices will yield the optimal configuration-space tour that visits the targets in the order specified by Step 1.

metric should be fast to compute – in particular, collisions are ignored at this stage – since the costs must be computed for all $m_1 + \sum_{i=1}^n m_i m_{i+1} + m_n$ graph edges.

Finally, we run a graph search algorithm to find the shortest path between the “Start” and “Goal” vertices. By construction, any path between the “Start” and “Goal” vertices will visit exactly one vertex in each layer, in the order specified by Step 1. Conversely, for any choice of IK solutions for the n targets, there will be a path in the graph between the “Start” and “Goal” vertices and going through the vertices representing these IK solutions. Therefore, Step 2 will find the *true optimal* selection of IK solutions that minimize the total cost, according to the specified configuration-space metric, given the order of the targets.

C. Complexity analysis

For Step 1, it is well-known that TSP is NP-complete, which means that finding the true optimal tour for n targets has in practice an exponential complexity. Many heuristics have been developed over the years to find near-optimal tours. For instance, *2-Opt* [13] and Lin-Kernighan-Helsgaun (LKH) [14] can find tours in practical times with an optimality gap below 5% and 1% respectively [15].

For Step 2, let M be an upper-bound of the number of IK solutions m_i per target. The number of graph vertices is then $\mathcal{O}(nM)$ and the number of the graph edges is $\mathcal{O}(nM^2)$. Since Dijkstra’s algorithm (with binary heap) has a complexity in $\mathcal{O}(|E| \log |V|)$ where $|E|$ and $|V|$ are respectively the number of edges and vertices, Step 2 has a complexity in $\mathcal{O}(nM^2 \log(nM))$.

For Step 3, one has to make $n-1$ queries to the motion planner, yielding a complexity in $\mathcal{O}(n)$. However, as the constant in the $\mathcal{O}()$ (average computation time per motion planning query) is large, the overall computation time is dominated by that of Step 3 in our setting. In general, the computation time of motion planning queries depends largely on the environment (obstacles), see [16], [17] for recent benchmarking results showing the CPU time required when planning practical robot motions.

IV. EXPERIMENTS

This section evaluates the proposed method when applied to the drilling task shown in Fig. 1. Our system is formed

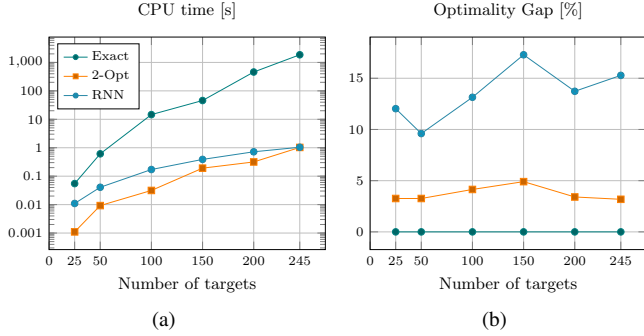


Fig. 4. Benchmarking results for three task-space TSP solvers. (a) CPU times for different number of targets. The Y axis is logarithmic (b) Task execution time for different number of targets. The sets of targets are selected randomly. The last sample considers all the 245 targets.

by a Denso VS060 6-DoF industrial manipulator equipped with a commercial off-the-shelf hand drill. All benchmarks were executed in a system with Intel[®] Core[™] i7 processor and 24 GB RAM, GeForce GTX 960M video card, running Ubuntu 16.04 (Xenial), 64 bits.

A. Benchmarking task-space TSP solvers

To solve the task-space TSP (Step 1 of our algorithm), one may use exact or near-optimal solvers. The choice depends on the trade-off between the available CPU time and the solution quality. Here we evaluate three TSP solvers.

- 1) *Exact*: Constraint Integer Programming (CIP) can be used to find true optimal TSP tour [15]. Here, we used the SCIP Optimization Suite [18] to implement an exact solver;
- 2) *2-Opt*: We re-implemented this simple, yet efficient, algorithm to find a near-optimal solution to TSP. The algorithm iteratively improves an initial guess by repeatedly replacing pairs of edges that cross over [15].
- 3) *RNN*: We re-implemented this algorithm, which consists in iteratively selecting the nearest neighbor as the next target to visit. This process is repeated until all the targets are visited [15]. One can do several *restarts* from different initial targets, and choose the tour with the lowest cost from all the restarts. The drawback of this method is that it tends to corner itself, which requires long edges to get back to unvisited targets.

Fig. 4 shows a benchmark of the three methods. We run the TSP solvers on task-space subsets of 25, 50, 100, 150, 200 random targets as well as on the total 245 targets. One can observe that the *2-Opt* solver yields high-quality tours (less than 5% of sub-optimality) with low CPU time usage (less than 1 s). As for the *Exact* solver, it is not practical for more than 150 targets. Therefore, for all the subsequent experiments, we shall use *2-Opt* as our near-optimal task-space TSP solver.

B. Benchmarking configuration-space metrics

The *configuration-space metric* that defines the edge cost in Step 2 of our algorithm is the key component for the

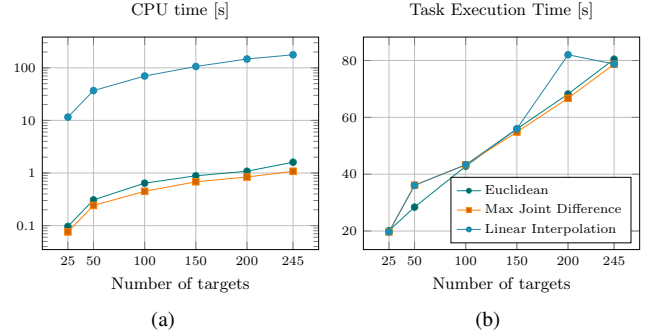


Fig. 5. Benchmarking results for three C-space metrics. (a) CPU times for different number of targets. The Y axis is logarithmic (b) Task execution time for different number of targets. The sets of targets are selected randomly. The last sample considers all the 245 targets.

overall performance of the method. Given two robot configurations \mathbf{q} and \mathbf{q}' , the ideal cost of the edge $c^*(\mathbf{q}, \mathbf{q}')$ is the duration of a time-optimal collision-free trajectory between them. However, since there are thousands of such edges, running full-fledged motion planning algorithms (with collision checks) for every edge would not be tractable. Therefore, one must consider approximate metrics, which should be fast to compute, yet give a good prediction of the corresponding time-optimal collision-free trajectory duration. Here we evaluate three such metrics.

- 1) *Weighted Euclidean joint distance*: The cost $c(\mathbf{q}, \mathbf{q}')$ is estimated as the weighted L^2 norm:

$$c(\mathbf{q}, \mathbf{q}') := \sqrt{\sum_{k=1}^{\text{DoF}} w_k (q'_k - q_k)^2},$$

where w_k is a positive weight for joint k . The weights are chosen in proportion to the maximum possible distance (Euclidean distance in the task-space) traveled by any point on the robot, when moving along the corresponding joint. Similar to [19], in our experiments this metric outperforms consistently the Euclidean joint distance.

- 2) *Maximum joint difference*: The cost $c(\mathbf{q}, \mathbf{q}')$ is estimated as follows:

$$c(\mathbf{q}, \mathbf{q}') := \max_k \left| \frac{q'_k - q_k}{\dot{q}_k^{\max}} \right|.$$

The intuition of this metric is to determine the maximum joint displacement when “moving” from \mathbf{q} to \mathbf{q}' by simply computing the joint difference, $(q'_k - q_k)$, over the joint k velocity limit, for $k \in [1, \dots, \text{DoF}]$. Then the maximum value is used;

- 3) *Linear trajectory interpolation*: the cost $c(\mathbf{q}, \mathbf{q}')$ is given by the duration of a trajectory obtained by linear interpolation. It only requires to specify the positions, \mathbf{q} and \mathbf{q}' , and guarantees continuity at the position level subject to the robot velocity and acceleration bounds. Moreover, this metric does not consider obstacles which greatly reduces its computing time.

Fig. 5 shows the benchmarking results for the three proposed configuration-space metrics. One can observe that the *Maximum joint difference* metric takes the lowest CPU time and yields task execution times comparable to, in some cases even better than, the *Euclidean* and *Linear Interpolation metrics*. Therefore, for all the subsequent experiments, we shall use *Maximum joint difference* as our metric.

C. Benchmarking discretization step size for the free DoF

Many industrial tasks such as spot-welding, spay-painting or drilling involve less than 6 degrees of freedom. Therefore, a classical 6-DoF industrial robot has more joints than strictly required to execute such tasks. Specifically, the drilling task at hand involves 5 DoF, since the rotation θ about the drilling direction is irrelevant. One approach to tackle this redundancy can consist in setting a specific value for the irrelevant DoF: for instance $\theta \in \{0, \frac{\pi}{2}, \pi, \frac{3\pi}{2}\}$ for a $\frac{\pi}{2}$ discretization step size. For each of the discretized value of θ , we then have a full 6-DoF IK problem. To solve the full 6-DoF IK, we next use OpenRAVE’s IKFast [20], which outputs all the IK solutions (here we have a “discrete” redundancy situation – think of the “elbow up” and “elbow down” configurations). We finally group all the IK solutions corresponding to all the discretized values of θ into a single list, which is the list of all IK solutions that will be considered for a given target. Table I gives the total number of IK solutions considered as a function of the discretization step size and of the number of targets.

TABLE I
NUMBER OF ROBOT CONFIGURATIONS DEPENDING ON THE DISCRETIZATION STEP SIZE AND THE NUMBER OF TARGETS

Step Size	Number of targets					
	25	50	100	150	200	245
π	235	538	1,044	1,548	2,071	2,495
$\frac{\pi}{2}$	344	816	1,598	2,368	3,094	3,779
$\frac{\pi}{3}$	481	1170	2,287	3,362	4,424	5,418
$\frac{\pi}{4}$	623	1,505	2,939	4,377	5,668	6,990
$\frac{\pi}{6}$	952	2,236	4,417	6,528	8,471	10,421
$\frac{\pi}{12}$	1,934	4,428	8,724	12,981	16,811	20,720

One can see that the choice of the *discretization step size* is governed by a trade-off between speed and optimality. Fig. 6 shows the computation time and task execution time as a function of the discretization step size. As expected, the computation time increases as the discretization step size decreases, but interestingly, the task execution time does not change significantly for step sizes below $\frac{\pi}{4}$, which thus yields a good trade-off between CPU time and task execution time. Therefore, for all the subsequent experiments, we shall use $\frac{\pi}{4}$ as our discretization step size.

D. Comparison to other methods

As none of the methods described in Section II provide public implementations, we were unable to reproduce their

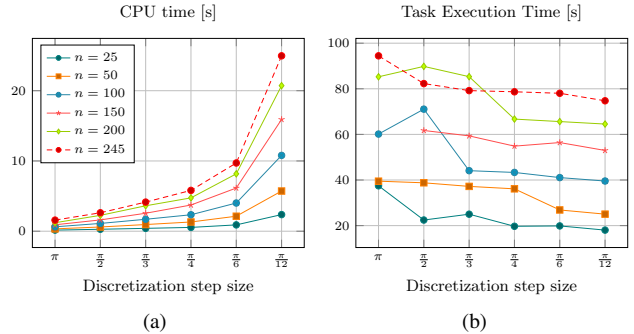


Fig. 6. Benchmarking results showing the effect of the discretization step size of the free DoF.

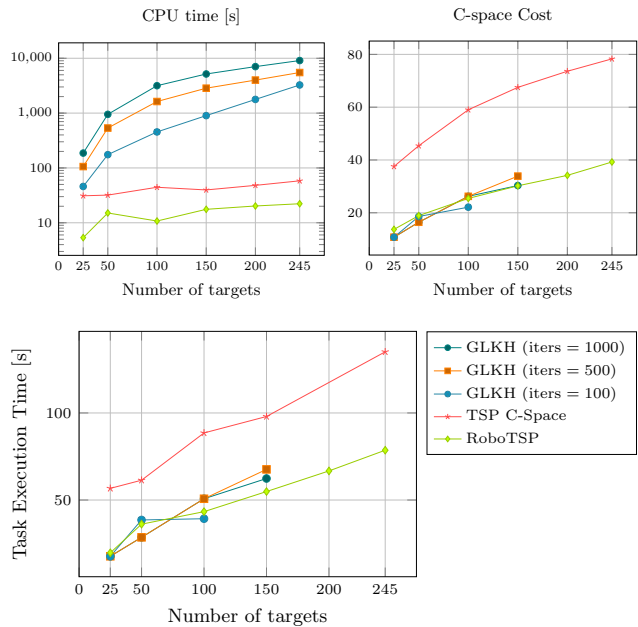


Fig. 7. Comparison of our method (*RoboTSP*) against other methods: i) Solved as TSP in configuration-space; ii) Solved as GTSP using GLKH.

results and perform a fair comparison with the method herein presented. However, we can note that the computation times reported in previous works are several orders of magnitude higher than ours, yet for problem instances that are smaller⁴ than what we consider in this work.

In the following, we compare our method to two of the existing methods, which we could re-implement.

- 1) *TSP in C-space* [3]: when only one configuration is considered per target, RTSP is reduced to a regular TSP in the configuration space. Here, for each target, we consider the IK solution with the best manipulability index [21];
- 2) *GLKH*: here the RTSP is formulated as a GTSP [5], [22], [23]. To solve that GTSP, we use the state-of-the-art GLKH solver [24] which makes use of the LKH

⁴The problem instance size is considered in terms of targets and configurations per target

heuristic [14].

Fig. 7 shows the comparison of our method (*RoboTSP*) to the two methods just described. While the *TSP in C-space* method has a similar running time as *RoboTSP* (indeed both run a TSP on the same number of targets), the time durations of the trajectories it produces are higher than those of *RoboTSP*, since it does not optimize the IK choice per target.

GLKH produces trajectories with similar total duration as *RoboTSP* but the computing time is higher several orders of magnitude.

A visualization with the trajectories produced by these three methods to visit all the 245 targets is available at <https://youtu.be/w33QfRjKFs8>.

V. CONCLUSIONS

We have proposed a method to determine a near-optimal sequence to visit n targets with multiple configurations per target, also known as the Robotic Task Sequencing Problem. For a complex drilling task, which requires visiting 245 targets with an average of 28.5 configurations per target, our method could compute a high-quality solution in less than a minute. To our knowledge, no existing approach could have solved the same problem in practical times. We have also provided a carefully benchmarked open-source software solution, which can be readily used in complex, real-world, applications such as drilling, spot-welding or spray-painting.

ACKNOWLEDGMENT

This work was supported in part by NTUitive Gap Fund NGF-2016-01-028 and SMART Innovation Grant NG000074-ENG.

REFERENCES

- [1] S. Alartartsev, S. Stellmacher, and F. Ortmeier, "Robotic Task Sequencing Problem: A Survey," *Journal of Intelligent & Robotic Systems*, vol. 80, no. 2, pp. 279–298, 2015.
- [2] L. L. Abdel-Malek and Z. Li, "The application of inverse kinematics in the optimum sequencing of robot tasks," *International Journal of Production Research*, vol. 28, no. 1, pp. 75–90, 1990.
- [3] Y. Edan, T. Flash, U. Peiper, I. Shmulevich, and Y. Sarig, "Near-minimum-time task planning for fruit-picking robots," *IEEE Transactions on Robotics and Automation*, vol. 7, no. 1, pp. 48–56, 1991.
- [4] M. Saha, G. Sanchez-Ante, and J.-C. Latombe, "Planning multi-goal tours for robot arms," in *IEEE International Conference on Robotics and Automation*, vol. 3. IEEE, 2003, pp. 3797–3803.
- [5] M. Saha, T. Roughgarden, J.-C. Latombe, and G. Sánchez-Ante, "Planning Tours of Robotic Arms among Partitioned Goals," *The International Journal of Robotics Research*, vol. 25, no. 3, pp. 207–223, 2006.
- [6] C. Chekuri, G. Even, and G. Kortsarz, "A greedy approximation algorithm for the group Steiner problem," *Discrete Applied Mathematics*, vol. 154, no. 1, pp. 15–34, 2006.
- [7] P. Zacharia and N. Aspragathos, "Optimal robot task scheduling based on genetic algorithms," *Robotics and Computer-Integrated Manufacturing*, vol. 21, no. 1, pp. 67–79, 2005.
- [8] E. K. Xidias, P. T. Zacharia, and N. A. Aspragathos, "Time-optimal task scheduling for articulated manipulators in environments cluttered with obstacles," *Robotica*, vol. 28, no. 03, p. 427, may 2010.
- [9] P. T. Zacharia, E. K. Xidias, and N. A. Aspragathos, "Task scheduling and motion planning for an industrial manipulator," *Robotics and Computer-Integrated Manufacturing*, vol. 29, no. 6, pp. 449–462, dec 2013.
- [10] E. Kolakowska, S. F. Smith, and M. Kristiansen, "Constraint optimization model of a scheduling problem for a robotic arm in automatic systems," *Robotics and Autonomous Systems*, vol. 62, no. 2, pp. 267–280, 2014.
- [11] J. Kuffner and S. LaValle, "RRT-connect: An efficient approach to single-query path planning," in *IEEE International Conference on Robotics and Automation (ICRA)*, vol. 2, 2000, pp. 995–1001.
- [12] Q.-C. Pham, "Trajectory Planning," in *Handbook of Manufacturing Engineering and Technology*. London: Springer London, 2015, pp. 1873–1887.
- [13] G. A. Croes, "A Method for Solving Traveling-Salesman Problems," *Operations Research*, vol. 6, no. 6, pp. 791–812, 1958.
- [14] K. Helsgaun, "An effective implementation of the Lin-Kernighan traveling salesman heuristic," *European Journal of Operational Research*, vol. 126, no. 1, pp. 106–130, oct 2000.
- [15] D. L. Applegate, R. E. Bixby, V. Chvatal, and W. J. Cook, *The Traveling Salesman Problem : a Computational Study*. Princeton University Press, 2011.
- [16] I. A. Sucan, M. Moll, and L. E. Kavraki, "The Open Motion Planning Library," *IEEE Robotics & Automation Magazine*, vol. 19, no. 4, pp. 72–82, 2012.
- [17] J. Meijer, Q. Lei, and M. Wisse, "Performance study of single-query motion planning for grasp execution using various manipulators," in *2017 18th International Conference on Advanced Robotics (ICAR)*. IEEE, 2017, pp. 450–457.
- [18] T. Achterberg, "SCIP: solving constraint integer programs," *Mathematical Programming Computation*, vol. 1, no. 1, pp. 1–41, jul 2009.
- [19] R. Bohlin and L. Kavraki, "Path planning using lazy PRM," in *IEEE International Conference on Robotics and Automation (ICRA)*. IEEE, 2000, pp. 521–528.
- [20] R. Diankov, "Automated Construction of Robotic Manipulation Programs," Ph.D. dissertation, Carnegie Mellon University, Robotics Institute, aug 2010.
- [21] T. Yoshikawa, "Manipulability of Robotic Mechanisms," *The International Journal of Robotics Research*, vol. 4, no. 2, pp. 3–9, jun 1985.
- [22] C. Wurll, D. Henrich, and H. Wörn, "Multi-Goal Path Planning for Industrial Robots," in *International Conference on Robotics and Application*, 1999.
- [23] C. Wurll and D. Henrich, "Point-to-point and multi-goal path planning for industrial robots," *Journal of Robotic Systems*, vol. 18, no. 8, pp. 445–461, 2001.
- [24] K. Helsgaun, "Solving the equality generalized traveling salesman problem using the Lin-Kernighan-Helsgaun Algorithm," *Mathematical Programming Computation*, vol. 7, no. 3, pp. 269–287, sep 2015.